Published in final edited form as:
J Mol Biol. 2008 March 28; 377(3): 882–888. doi:10.1016/j.jmb.2008.01.025.

Determination of the Transition-State Entropy for Aggregation Suggests How the Growth of Sickle Cell Hemoglobin Polymers can be Slowed

Peter G. Vekilov[1,2,*], **Oleg Galkin**[1], **B. Montgomery Pettitt**[2], **Nihar Choudhury**[2], and **Ronald L. Nagel**[3]

1 *Department of Chemical and Biomolecular Engineering, University of Houston, Houston, TX 77204, USA*

2 *Department of Chemistry, University of Houston, Houston, TX 77204, USA*

3 *Department of Medicine (Division of Hematology), Albert Einstein College of Medicine, The Bronx, NY 10461, USA*

Abstract

Sickle cell anemia is associated with the mutant hemoglobin HbS, which forms polymers in red blood cells of patients. The growth rate of the polymers is several micrometers per second, ensuring that a polymer fiber reaches the walls of an erythrocyte (which has a 7-μm diameter) within a few seconds after its nucleation. To understand the factors that determine this unusually fast rate, we analyze data on the growth rate of the polymer fibers. We show that the fiber growth follows a first-order Kramers-type kinetics model. The entropy of the transition state for incorporation into a fiber is 95 J mol^{-1} K^{-1}, very close to the known entropy of polymerization. This agrees with a recent theoretical estimate for the hydrophobic interaction and suggests that the gain of entropy in the transition state is due to the release of the last layer of water molecules structured around contact sites on the surface of the HbS molecules. As a result of this entropy gain, the free-energy barrier for incorporation of HbS molecules into a fiber is negligible and fiber growth is unprecedentedly fast. This finding suggests that fiber growth can be slowed by components of the red cell cytosol, native or intentionally introduced, which restructure the hydration layer around the HbS molecules and thus lower the transition state entropy for incorporation of an incoming molecule into the growing fiber.

Keywords

sickle cell anemia; hemoglobin S polymerization; growth rate; hydration layer; transition-state entropy

Introduction

Polymerization of sickle cell hemoglobin, HbS, is one of the basic events in the pathophysiology of sickle cell anemia.[1,2] It occurs in the venous circulation,[3] when HbS is in deoxy state and in its R conformation. HbS polymerization is a first-order phase transformation,[4] and it follows a pathway common for all such transformations: after discrete events of

*Corresponding author. Department of Chemical and Biomolecular Engineering, University of Houston, Houston, TX 77204, USA. E-mail address: vekilov@uh.edu.
Edited by M. Levitt
Present addresses: O. Galkin, Physical Optics Corporation, 20600 Gramercy Place, Building 100, Torrance, CA 90501-1821, USA; N. Choudhury, Theoretical Chemistry Section, Chemistry Group, Bhabha Atomic Research Centre, Mumbai 400 085, India.

nucleation of polymer fibers, they grow by incorporating single molecules from solution.[5–8] The typical growth rates of an HbS polymer fiber are of the order of several micrometers per sec ond,[9,10] so that a polymer fiber reaches the cell walls within a few seconds after nucleation.[8,10] The resulting deformation and damage of the cell membrane are among the major events in the disease pathophysiology.[11,12] Slower growth would allow cells with nucleated polymers to reach the arterial circulation undamaged, where hemoglobin is in its T state and does not polymerize, while the polymers formed in the venous circulation dissolve. In this article, we analyze the mechanisms of incorporation of HbS molecules into growing polymer fibers and suggest potential means to slow the fiber growth.

Results and Discussion

Kinetic model of HbS polymer fiber growth

The growth kinetics of HbS can be quantified by direct monitoring of a supersaturated solution of HbS in a way that allows detection of individual, nucleated, growing fibers. The solution composition mimics the composition of the red cell cytosol: the solution contains only 0.15 M phosphate buffer at pH 7.35, 0.05 M sodium dithionite to facilitate deoxygenation,[9] and hemoglobin S with concentration from 200 to 230 mg ml^{-1}. These HbS concentrations are lower than those in the red cells, where they are around 350 mg ml^{-1}; on the other hand, we carry out the experiments in completely deoxygenated conditions, while there is significant oxygen pressure in the venous circulation. With these caveats, we view the growth rates measured in our setup as representative for the HbS fiber growth rates in the red cells. The solution is held in a thin slide, and individual fibers as short as 0.5–1 μm are detected at the times of their appearance. Their length can be determined in subsequent times. The procedure for determination of the fiber growth rate, *R*, from sequences of images of the evolution of HbS polymerization and other experimental details are discussed in Ref. 13. In the same article, it was shown that due to the slow diffusive supply of HbS molecules from the solution to the growing end of a fiber, the average growth rate of the HbS fibers is reduced,[14] in comparison to the case of oversupply of material, by a factor $\kappa \approx 3$.

The fiber growth rates *R* in Fig. 1a are 2–4 μm s^{-1}. Since human red cells have a diameter of about 7 μm, if similar rates are found in the red cells of patients with sickle cell anemia, the fibers would reach the cell walls and stretch the cells within 2–3 s. These rates are faster by at least a factor of 10× than the fastest rate recorded for the growth of any protein ordered structure and 100× and 1000× faster than the typical values of these rates.[15] To a certain extent, this fast kinetics is due to the high concentration of HbS. To identify the additional factors that contribute to the fast growth rate and those that could help control and slow the growth, we need to understand the mechanism of incorporation of the HbS molecules into the fibers and the nature and magnitude of the respective free-energy barriers. For this, we develop a testable model of the incorporation.

The growth rate *R* is proportional to the net number of molecules that join a growth site at the growing end of a fiber per unit time

$$R=b(j_+ - j_-), \tag{1}$$

where b=5.5 nm is the effective diameter of an HbS molecule, j_+ is the number of molecules entering a growth site, and j_- is the number of molecules departing from a growth site per unit time. A growth site is a location at which an incoming molecule has half of the number of neighbors inside the polymer.[16,17] Equation (1) assumes that the density of growth sites is high, equal to 1, and that their creation is not a kinetic obstacle. In view of the HbS polymer structure, where the 14 molecules in a cross section are at different heights[18] (Fig. 2a), this is a natural assumption.

The incoming flux into a site is $j_+ = \hat{J}\Delta S_{site} \approx \hat{J}b^2$, where ΔS_{site} is the area of the cross section of the fiber per growth site. Thus, we evaluate the flux $\hat{J}$ of molecules with concentration n that, driven by a concentration gradient, overcome a barrier to reach the surface. The barrier is due to the interaction of an incoming HbS molecule with the HbS molecules at the surface of the fiber. We denote with $U(x)$ the potential of the mean force of this interaction. $U(x)$ has a repulsive part, as discussed below, and an attractive part due to the hydrophobic forces that keep the HbS molecules in the fiber together. These hydrophobic contacts are formed between valine of one HbS molecule (the mutation from glutamate, an acidic amino acid residue in normal adult hemoglobin, to valine in HbS is the crucial mutation underlying sickle cell anemia) and alanine, phenylalanine, and leucine from an adjacent HbS molecule.[19–22] In Fig. 2b, the resulting free-energy relief $U(x)$ is schematically depicted as a function of the distance x from the fiber-growing surface. The potential of the mean force reaches its maximum value $\Delta G^{\neq}$ at the crossing of the increasing and receding branches. This $\Delta G^{\neq} = \Delta H^{\neq} - T\Delta S^{\neq}$, and it represents the free energy of the transition state, that is, the barrier for incorporation, whose enthalpy, $\Delta H^{\neq}$, and entropy, $\Delta S^{\neq}$, components are discussed below.

To evaluate $\hat{J}$, we use the generalized Fick's law, $\hat{J} = (\hat{a}D/k_BT)d\mu/dx$, with $\mu(T,x) = \mu_0(T) + k_BT\ln[\hat{a}(x)] + U(x)$, where $\hat{a}$ is the HbS activity. This transforms to:[23,24]

$$\widehat{J} = D\left[\frac{d\widehat{a}(x)}{dx} + \widehat{a}(x)\frac{d(U(x)/k_BT)}{dx}\right],\ x>0. \tag{2}$$

Equation (2) is often referred to as the Smoluchowski equation.[25]

We represent $U(x)$ around its maximum with a symmetric function and introduce the parameter Λ as the radius of curvature of $U(x)/k_BT$ at this maximum:[26]

$$\Lambda = (1/2\pi \parallel \partial^2(U/k_BT)/\partial x^2\parallel_{max})^{-1/2}. \tag{3}$$

The end of a single 14-member growing fiber can be considered as a point sink for HbS molecules, supplied by the entire three-dimensional space around it. The integration of Eq. (2) for this case should be carried out in three dimensions. However, the data in Fig. 1a were collected with fiber bundles, which were several micrometers thick. Thus, each individual fiber inside this bundle is only supplied from the solution space immediately in its front, and a one-dimensional integration of Eq. (2) is appropriate.

We position the x-axis along the fiber axis (Fig. 2b) and place its beginning, $x=0$, at the location of the $U(x)$ maximum. In search of a steady $\hat{J}$ =const, we integrate Eq. (2) with two sets of boundary conditions:

1. At a distance δ from the surface, $x \geq \delta$ and $U=0$, and the HbS activity is $\hat{a}_\delta$. If there were no constraints due to the diffusion of HbS toward the growing end of a fiber, $\hat{a}_\delta$ would be equal to $\hat{a}$ in the solution bulk (Fig. 2c). However, because of the slow diffusion, $(\hat{a}_\delta - \hat{a}_e) = \kappa^{-1}(\hat{a} - \hat{a}_e)$.[9] The distance δ is chosen such that it is longer than the range of interaction of the solute molecules with the surface, which can be a few solvent molecular sizes, that is, 1 nm, and is shorter than the distances between the HbS molecules in the solution, $n^{-1/3} \approx 8$ nm. Since the rate of diffusion over a sharp barrier only depends on the curvature around the maximum,[24,27] the choice of δ does not affect the result.
2. In the fiber, that is, at $x \leq 0$, $\hat{a}$ =0.

With these two boundary conditions, the integration yields

$$\widehat{J}=D/\Lambda\exp(-\Delta G^{\neq}/k_{\mathrm{B}}T)\widehat{a}_{\delta}. \tag{4}$$

In equilibrium, both $\hat{a}$ and $\hat{a}_{\delta}$ equal the solubility $\hat{a}_{\mathrm{e}}$, and $j_+ = j_-$. Since j_- does not depend on $\hat{a}$, and with b^3 =Omega;, the volume that one HbS molecule occupies in the fiber, the growth rate R is

$$\begin{aligned} R=b(j_+ - j_-)&=\Omega\frac{D}{\Lambda}\exp\left(-\frac{\Delta G^{\neq}}{k_{\mathrm{B}}T}\right)(\widehat{a}_{\delta}-\widehat{a}_{e})\\ &=\frac{\Omega\widehat{a}_{e}D}{\Lambda}\exp\left(\frac{\Delta S^{\neq}}{k_{\mathrm{B}}}\right)\exp\left(-\frac{\Delta H^{\neq}}{k_{\mathrm{B}}T}\right)[\exp(\Delta\mu_{\delta}/k_{\mathrm{B}}T)-1]\\ &=\kappa^{-1}\frac{\Omega\widehat{a}_{e}D}{\Lambda}\exp\left(\frac{\Delta S^{\neq}}{k_{\mathrm{B}}}\right)\exp\left(-\frac{\Delta H^{\neq}}{k_{\mathrm{B}}T}\right)[\exp(\Delta\mu/k_{\mathrm{B}}T)-1]. \end{aligned} \tag{5}$$

In Eq. (5), $[\exp(\Delta\mu_{\delta}/k_{\mathrm{B}}T)-1]=\hat{a}_{\delta}/\hat{a}_{\mathrm{e}}-1=\kappa^{-1}[\hat{a}/\hat{a}_{\mathrm{e}}-1]=\kappa^{-1}[\exp(\Delta\mu\delta/k_{\mathrm{B}}T)-1]$ is the driving force for polymerization. With this, Eq. (5) has the typical form for a first-order chemical rate law.28 According to the Stokes–Einstein expression, $D=k_{\mathrm{B}}T/3\pi\eta b$, where η is the solution viscosity.29,30 The reciprocal dependence between R and η makes Eq. (5) similar to a Kramers-type kinetics law,31,32 as should be expected for a reaction in solution. The product $\Omega\hat{a}_{\mathrm{e}}$ accounts for the change in molecular concentration of HbS between the solution and the fiber.

Does the model apply to HbS fiber growth?

The parameters $\Delta G^{\neq}$, $\Delta H^{\neq}$, $\Delta S^{\neq}$, and Δ characterize the potential of interaction $U(x)$ between an incoming molecule and the fiber edge. Since a hemoglobin molecule carries around 0.5 to 1 elementary charge at the pH of the HbS polymerization experiments (pH 7.35), adjusted to that of the blood, $U(x)$ is likely of nonelectrostatic origin. Numerous recent experimental[33–37] and theoretical[38–41] works have shown that a several-angstrom-thick solvent layer exists around protein molecules. Within this hydration layer,[37,42] the water molecules are in either of two states, between which a dynamic equilibrium exists: directly attached to the protein surface and “free.” Another equilibrium exists between the hydration layer and the bulk solution water.[37] This layer determines the thermodynamics and kinetics of enzyme–substrate and DNA–drug binding.[43,44] It has been demonstrated that enthalpy and entropy contributions from the solvent layer largely determine the thermodynamics of crystallization of several proteins.[45–49] It has also been shown that the dynamics of the water molecules within the hydration layer and of exchange between the layer and the bulk water determine the kinetics of incorporation into crystals.[26,50,51] In view of the hydrophobic contacts between the mutated β6 valine and the alanine, phenylalanine, and leucine from an adjacent HbS molecule,[19–22] it is natural to assume that the water structure dynamics will also constitute the main component of the barriers for incorporation of HbS molecules into fibers.

For molecules whose aggregation is hampered by a hydration layer, $\Delta H^{\neq}$ mostly represents the energy of the interactions (hydrogen bonds and van der Waals) inside this hydration layer, which are broken when the hydration water is pushed out of the contact site between two adjacent molecules.[52–56] Remarkably, $\Delta H^{\neq}$ for about 10 diverse substances, ranging from inorganic salts, to organic molecular compounds, to proteins and viruses, was found to be within a narrow range centered on 30 kJ $\mathrm{mol}^{\neq 1}$.[57] This consistency of $\Delta H^{\neq}$ suggests that the barrier is determined by the removal of a small number of water molecules at the contact site, even for molecules as large as viruses. Correspondingly, the width Λ was found to be of the order of several water molecules, that is, from 0.6 to 1 nm.[34,37,47,55,58,59] If the barrier for incorporation of HbS molecules into HbS fibers is of similar origin, we expect similar values for $\Delta H^{\neq}$ and Λ.

To test if Eq. (5) and the assumptions behind it apply to the growth of HbS polymer fibers, in Fig. 1b, we replotted the data from Fig. 1a in Arrhenius coordinates, corresponding to the rate

law in Eq. (5). The chemical potential difference $\Delta\mu$ and the activity $\hat{a}$ were calculated for each HbS concentration and temperature using six virial coefficients B_i for HbS as in Ref. 60. Using temperature-dependent $\hat{a}_e = \gamma C_e$ and $\Delta\mu$ accounts for the dependence of HbS solubility on temperature.18 The factor κ^{-1} in Eq. (5) accounts for the depletion of HbS concentration near the fiber edge. The data in Fig. 1b fit a straight line, which supports the applicability of Eq. (5).

To additionally test the validity of the model behind Eq. (5), we evaluate the parameters of this model from the slope and intercept of the straight line in Fig. 1b. Since the viscosity η decreases with increasing temperature, D in Eq. (5) is a function of temperature, $D=D_o\exp(-E_\eta/k_BT)$, where E_η is the effective Arrhenius activation energy for η. For water and low-concentration buffers, E_η is ~ 15 kJ mol^{-1}.[61] With this E_η, D_0 =1.4×10^{-4} cm^2 s^{-1}. In view of the temperature dependence of D, the slope of the straight line in Fig. 1b corresponds to $\Delta H^{\neq}+E_\eta$. From the data in Fig. 1b, $\Delta H^{\neq}+E_\eta$ =43 kJ mol^{-1}, so that $\Delta H^{\neq}$=28 kJ mol^{-1}. This value is within the range found for other species forming ordered solid phases from solution. This correspondence supports the applicability of Eq. (5) to the growth of HbS polymers, and the suggestion that the activation barrier for incorporation of HbS molecules into a growing fiber characterizes the rearrangement of the water shell at the contact surfaces of the HbS molecules.

The transition-state entropy and the free-energy barrier for incorporation

The intercept of the straight line in Fig. 1b is equal to $\ln(D_0/\Lambda)+\Delta S^{\neq}/k_B$. Prompted by the agreement between the value of $\Delta H^{\neq}$ for HbS polymerization and the expectations from a hydration model, we take Λ=1 nm. With the above value for D_0, we obtain $\Delta S^{\neq}$=95 J mol^{-1} K^{-1}.

The transition-state entropy $\Delta S^{\neq}$ contains two contributions: from the loss of rotational and translational degrees of freedom of the incoming molecule and from the loss or gain of rotational and translational degrees of freedom of water molecules. The HbS contribution is always negative. The loss of rotational degrees of freedom in the transition state is equivalent to selecting a molecular orientation suitable for incorporation into the fiber. This entropy has been estimated and found to be of the order −50 J mol^{-1} K^{-1} for protein molecules.[62] The water molecule contribution may be negative or positive, depending on whether additional water molecules are trapped between the incoming HbS molecule and the fiber edge or some of those associated to the HbS molecules in the solution and to the fiber edge are released.[45,46] Estimates are that the release of one water molecule contributes ~ 20 J mol^{-1} K^{-1}[45,48,63,64] to the total entropy of the transition state. In general, depending on the sign and magnitude of the water contribution, the total $\Delta S^{\neq}$ may be either positive or negative.

The positive sign of the total $\Delta S^{\neq}$ determined from the data in Fig. 1b indicates that the entropy gain stemming from the release of associated water is greater in magnitude than the entropy loss of the HbS molecule. The entropy contribution to the free-energy barrier for incorporation into the HbS polymer fiber lowers this barrier and accelerates the growth of the polymer. Furthermore, the obtained value for $\Delta S^{\neq}$ is close to the value of the standard entropy for HbS polymerization, ΔS^o, which, at 25°C, is 103 J mol^{-1} K^{-1}.[18] Both of these facts agree with an evaluation, using molecular dynamics, of the thermodynamic parameters, ΔG, ΔH, and ΔS, of the hydrophobic interaction between two flat graphene sheets of 60 carbon atoms each, or an interface of ~ 130 Å^2, approaching each other in water (Fig. 3).[55,65,66] The agreement indicates that the positive value of $\Delta S^{\neq}$ reflects the gain of degrees of freedom of the water molecules, which are associated to the HbS molecules in the solution and are set free upon the formation of the transition state and the subsequent incorporation.[54,56,67] Such gain is expected for the hydrophobic contacts that form between the valine at the β6 site and the alanine, phenylalanine, and leucine from the adjacent HbS molecules.[19–22] The magnitude of $\Delta S^{\neq}$ resulting from the simulations, obtained from the value of $T\Delta S \approx 7.5$ kJ mol^{-1} in Fig.

3 at 298 K, is ~ 25 J mol^{-1} K^{-1} per C–C pair.[55] This is lower in magnitude than the value of $\Delta S^{\neq}$ for incorporation of HbS molecules into a growing fiber, indicating the participation of several atoms from the two adjacent HbS molecules in the hydrophobic contact in the fiber. The similarity between $\Delta S^{\neq}$ and ΔS^{o} cannot be used to judge for or against a drying transition as the gap between the contact sites on the incoming HbS molecules and resident HbS molecules in the fiber shrinks: in the case of a drying, $\Delta S^{\neq}$ would be associated with the last layer of water removed from the gap. However, since the hydrophobic contact sites on the HbS molecules have relatively small area,[19–22] it is unlikely that drying out occurs.

From the values of $\Delta H^{\neq}$ and $\Delta S^{\neq}$, the transition-state free energy $\Delta G^{\neq}$ is negligible; that is, the entropy and enthalpy contributions to the incorporation barrier cancel out and incorporation is effectively barrier free. Note that $\Delta H^{\neq}$ and $\Delta S^{\neq}$ are never negligible. This value of $\Delta G^{\neq}$ indicates that the fast growth of the HbS polymer fibers is due to the strong structuring of the water molecules around the HbS in solution, yielding a high value for the transition-state entropy $\Delta S^{\neq}$ when they are released during incorporation into the fibers.

There is very limited data on $\Delta S^{\neq}$ for other aggregating systems. Results on the kinetics of adsorption of the ions of $NH_4H_2PO_4$ on the surface of a crystal of this material indicate that the rate of adsorption is well modeled by $(D/\Lambda)\exp(\Delta S^{\neq}/k_B)\exp(-H^{\neq}/k_BT)$.59,68 Arrhenius plots of the data yielded $\Delta H^{\neq}$=28 kJ mol^{-1}. Using independently determined D yielded Λ=13 Å,[59] very close to expectations from the water shell model. This suggests that $\Delta S^{\neq} \sim 0$, likely as a result of the compensation of its two components.

Clinical implications and open questions

The large positive value of the transition-state entropy for the incorporation of HbS molecules into fibers suggests that if $\Delta S^{\neq}$ could be lowered, this could slow the rate of fiber growth and, in this way, prevent the disastrous consequences of HbS polymerization. Indeed, bringing down $\Delta S^{\neq}$ to 50 J mol^{-1} K^{-1} would slow the rate of fiber growth by a factor of ~ 5000×, from a few micrometers per second to a few micrometers per hour. The consequences for the disease pathophysiology would be that even if HbS polymers nucleate in the erythrocyte cytosol, the fibers would not grow to a size comparable to that of the cell, ~7 μm, for the ~10 s that red blood cells spend in the low-oxygen environment in the venous circulation. The caveat is that growth regulation via rearrangement of water structures has been accomplished for just two systems.[51,69] In the case of insulin crystallization,[70] regulation required significant amounts of the active additive[69]; in the case of calcite growth, nanomolar amounts of additives were used, but they only led to effects of less than 2× on the growth rate. Still, the structuring of water around protein molecules in solution is an area of active research, and it is likely that insights will be produced, which may lead to suggestions for suppression of the growth of the HbS polymers.[37]

A tantalizing hypothesis is that hydroxyurea is active in such rearrangement. Hydroxyurea is used in patients with sickle cell anemia and in those with thrombocytosis. Its chemical similarity to a known osmolyte, urea, could explain the beneficial effects of hydroxyurea, evident in patients before fetal hemoglobin expression is enhanced.[71] (Expression of fetal hemoglobin and the resulting dilution of HbS in the red cell are viewed as the greatest benefits of the hydroxyurea treatment for sickle cell anemia[72,73]). Urea denatures proteins by rearranging the water involved in the hydrophobic attraction;[74,75] thus, the hypothesis that hydroxyurea may have similar effects is not unfounded. One could imagine that other osmolytes could similarly change the rate of attachment to an HbS fiber by changing the free-energy barrier for association.

Acknowledgements

This work was supported by the Welch Foundation (Grant Numbers E-1641 and E-1028) and the National Institutes of Health (Grant Numbers G091474 and GM37657). We thank Jesse Howard for help in preparing Fig. 3.

Abbreviation used

HbS

sickle cell hemoglobin

References

1. Stuart MJ, Nagel RL. Sickle-cell disease. Lancet 2004;364:1343–1360. [PubMed: 15474138]
2. Sergeant GR. Sickle-cell disease. Lancet 1997;350:725–730. [PubMed: 9291916]
3. Hahn EV, Gillespie EB. Sickle cell anemia: report of a case greatly improved by splenectomy. Experimental study of sickle cell formation. Arch Int Med 1927;39:233–254.
4. Hofrichter H, Ross PD, Eaton WA. Kinetics and mechanism of deoxyhemoglobin S gelation: a new approach to understanding sickle cell disease. Proc Natl Acad Sci USA 1974;71:4864–4868. [PubMed: 4531026]
5. Ferrone FA, Hofrichter H, Eaton WA. Kinetics of sickle cell hemoglobin polymerization. I Studies using temperature jump and laser photolysis techniques. J Mol Biol 1985;183:591–610. [PubMed: 4020872]
6. Ferrone FA, Hofrichter H, Eaton WA. Kinetics of sickle cell hemoglobin polymerization. II A double nucleation mechanism. J Mol Biol 1985;183:611–631. [PubMed: 4020873]
7. Samuel RE, Guzman AE, Briehl RW. Kinetics of hemoglobin polymerization and gelation under shear: II The joint concentration and shear dependence of kinetics. Blood 1993;82:3474–3481. [PubMed: 8241514]
8. Briehl RW. Nucleation, fiber growth and melting and domain formation and structure in sickle cell hemoglobin gels. J Mol Biol 1995;245:710–723. [PubMed: 7844835]
9. Galkin O, Nagel RL, Vekilov PG. The kinetics of nucleation and growth of sickle cell hemoglobin fibers. J Mol Biol 2007;365:425–439. [PubMed: 17069853]
10. Jones CW, Wang JC, Ferrone FA, Briehl RW, Turner MS. Interactions between sickle hemoglobin fibers. Faraday Discuss 2003;123:221–236. [PubMed: 12638863]
11. Embury SH. The not-so-simple process of sickle cell vasoocclusion. Microcirculation 2004;11:101–113. [PubMed: 15280086]
12. Eaton WA. Linus Pauling and sickle cell disease. Biophys Chem 2003;100:109–116. [PubMed: 12646356]
13. Galkin O, Pan W, Filobelo L, Hirsch RE, Nagel RL, Vekilov PG. Two-step mechanism of homogeneous nucleation of sickle cell hemoglobin polymers. Biophys J 2007;92:902–913. [PubMed: 17449671]
14. Vekilov PG, Thomas BR, Rosenberger F. Effects of convective solute and impurity transport on protein crystal growth. J Phys Chem, B 1998;102:5208–5216.
15. Vekilov PG. What determines the rate of growth of crystals from solution? Cryst Growth Des 2007;7:2796–2810.
16. Kossel W. Zur Theorie des Kristallwachstums. Nachr Ges Wiss Götingen 1928:135–138.
17. Stranski IN. Zur Theorie des Kristallwach-stums. Z Phys Chem 1928;136:259–278.
18. Eaton, WA.; Hofrichter, J. Sickle cell hemoglobin polymerization. In: Anfinsen, CB.; Edsal, JT.; Richards, FM.; Eisenberg, DS., editors. Advances in Protein Chemistry. 40. Academic Press; San Diego, CA: 1990. p. 63-279.
19. Wishner B, Ward K, Lattman E, Love W. Crystal structure of sickle-cell deoxyhemoglobin at 5 Å resolution. J Mol Biol 1975;98:179–194. [PubMed: 1195378]
20. Fronticelli C, Gold R. Conformational relevance of the beta6Glu replaced by Val mutation in the beta subunits and in the beta(1–55) and beta(1–30) peptides of hemoglobin S. J Biol Chem 1976;251:4968–4972. [PubMed: 956170]

21. Dykes GW, Crepeay RH, Edelstein SJ. Three-dimensional reconstruction of 14-filament fibers of hemoglobin S. J Mol Biol 1979;130:451–472. [PubMed: 480359]
22. Carrager B, Bluemke DA, Gabriel B, Potel MJ, Josephs R. Structural analysis of polymers of sickle cell hemoglobin. I Sickle cell hemoglobin fibers. J Mol Biol 1988;199:315–331. [PubMed: 3351926]
23. Smoluchowski M. Drei Vorträge uber Diffusion, Brownsche Bewegung und Koagulation von Kolloidteilchen. Phys Z 1916;17:557–585.
24. Zel'dovich YB. Theory of new phase formation: cavitation. Acta Physicochim URSS 1943;18:1–22.
25. Coffey, W. Development and application of the theory of Brownian motion. In: Evans, MW., editor. Advances in Chemical Physics. 63. John Wiley and Sons, Inc; Hoboken, NJ: 1985. p. 69-252.
26. Petsev DN, Chen K, Gliko O, Vekilov PG. Diffusion-limited kinetics of the solution–solid phase transition of molecular substances. Proc Natl Acad Sci USA 2003;100:792–796. [PubMed: 12552115]
27. von Smoluchowski M. Versuch einer mate-matischen theorie der koagulationskinetik kollpider losungen. Z Phys Chem 1918;92:129–135.
28. Eyring, H.; Lin, SH.; Lin, SM. Basic Chemical Kinetics. John Wiley and Sons; New York, NY: 1980.
29. Berry, PS.; Rice, SA.; Ross, J. Physical Chemistry. 2. Oxford University Press; New York, NY: 2000.
30. Einstein A. Zur Theorie der Brownschen Bewegung. Ann Phys 1906;19:371–381.
31. Kramers HA. Brownian motion in a field of force and the diffusion model of chemical reactions. Physica A 1940;7:284–304.
32. Hänggi P, Talkner P, Borkovec M. Reaction-rate theory: fifty years after Kramers. Rev Mod Phys 1990;62:251–341.
33. Svergun DI, Richard S, Koch MH, Sayers Z, Kuprin S, Zaccai G. Protein hydration in solution: experimental observation by x-ray and neutron scattering. Proc Natl Acad Sci USA 1998;95:2267–2272. [PubMed: 9482874]
34. Leckband D, Israelachvili J. Intermolecular forces in biology. Q Rev Biophys 2001;34:105–267. [PubMed: 11771120]
35. Raviv U, Klien J. Fluidity of bound hydration layers. Science 2002;297:1540–1543. [PubMed: 12202826]
36. Ball P. Chemical physics: how to keep dry in water. Nature 2003;423:25–26. [PubMed: 12721610]
37. Pal SK, Zewail AH. Dynamics of water in biological recognition. Chem Rev 2004;104:2099–2124. [PubMed: 15080722]
38. Lounnas V, Pettitt BM, Findsen L, Subramanian S. A microscopic view of protein solvation. J Phys Chem 1992;96:7157–7158.
39. Lounnas V, Pettitt BM. A connected-cluster of hydration around myoglobin: correlation between molecular dynamics simulations and experiment. Proteins: Struct Funct Genet 1994;18:133–147. [PubMed: 8159663]
40. Lounnas V, Pettitt BM, Phillips NG. A global model of the protein–solvent interface. Biophys J 1994;66:601–614. [PubMed: 8011893]
41. Makarov V, Andrews KA, Pettitt BM. Protein hydration density: theory simulation and crystallography. Curr Opin Struct Biol 1998;8:218–221. [PubMed: 9631296]
42. Bhattacharyya SM, Wang ZG, Zewail AH. Dynamics of water near a protein surface. J Phys Chem, B 2003;107:13218–13228.
43. Chalikian TV, Plum GE, Sarvazyan AP, Breslaver KJ. Influence of drug binding on DNA hydration: acoustic and densimetric characterizations of netropsin binding to the poly(dAdT)·poly(dAdT) and poly(dA)·poly(dT) duplexes and the poly(dT)·poly(dA)·poly(dT) triplex at 25°C. Biochemistry 1994;33:8629–8640. [PubMed: 8038152]
44. Chalikian TV, Völker J, Srinivasan AR, Olson WK, Breslauer KJ. The hydration of nucleic acid duplexes as assessed by a combination of volumetric and structural techniques. Biopolymers 1999;50:459–471. [PubMed: 10479730]
45. Derewenda ZS, Vekilov PG. Entropy and surface engineering in protein crystallization. Acta Crystallogr, Sect D: Biol Crystallogr 2006;62:116–124. [PubMed: 16369101]

46. Vekilov, PG. Solvent entropy effects in the formation of protein solid phases. In: Carter, CW., Jr; Sweet, RM., editors. Methods in Enzymology, Volume 368: Macromolecular Crystallography, Part C. Academic Press; San Diego, CA: 2003. p. 84-105.
47. Petsev DN, Wu X, Galkin O, Vekilov PG. Thermodynamic functions of concentrated protein solutions from phase equilibria. J Phys Chem, B 2003;107:3921–3926.
48. Bergeron L, Filobelo L, Galkin O, Vekilov PG. Thermodynamics of the hydrophobicity in crystallization of insulin. Biophys J 2003;85:3935–3942. [PubMed: 14645082]
49. Vekilov PG, Feeling-Taylor AR, Yau ST, Petsev DN. Solvent entropy contribution to the free energy of protein crystallization. Acta Crystallogr, Sect D: Biol Crystallogr 2002;58:1611–1616. [PubMed: 12351872]
50. Vekilov, PG.; Chernov, AA. The physics of protein crystallization. In: Ehrenreich, H.; Spaepen, F., editors. Solid State Physics. 57. Academic Press; New York: 2002. p. 1-147.
51. Elhadj S, De Yoreo JJ, Hoyer JR, Dove PM. Role of molecular charge and hydrophilicity in regulating the kinetics of crystal growth. Proc Natl Acad Sci USA 2006;103:19237–19242. [PubMed: 17158220]
52. Kauzmann, W. Some forces in the interpretation of protein denaturation. In: Anfinsen, CB.; Anson, ML.; Bailey, K.; Edsall, JT., editors. Advances in Protein Chemistry. 14. Academic Press; New York, NY: 1959. p. 1-63.
53. Tanford, C. The Hydrophobic Effect: Formation of Micelles and Biological Membranes. John Wiley and Sons; New York, NY: 1980.
54. Chandler D. Two faces of water. Nature 2002;417:491. [PubMed: 12037545]
55. Choudhury N, Pettitt BM. Enthalpy–entropy contributions to the potential of mean force of nanoscopic hydrophobic solutes. J Phys Chem, B 2006;110:8459–8463. [PubMed: 16623532]
56. Chandler D. Interfaces and the driving force of hydrophobic assembly. Nature 2005;437:640–647. [PubMed: 16193038]
57. De Yoreo, JJ. Eight Years of AFM: What has it taught us about Solution Crystal Growth. 13th International Conference on Crystal Growth; Kyoto, Japan. 2001.
58. Vekilov, PG. Kinetics and mechanisms of protein crystallization at the molecular level. In: Vo-Dinh, T., editor. Methods in Molecular Biology, Volume 300: Protein Nanotechnology, Protocols, Instrumentation, and Applications. Humana Press; Totowa, NJ: 2005. p. 15-52.
59. Vekilov PG, Kuznetsov YG, Chernov AA. The effect of temperature on step motion; (101) ADP face. J Cryst Growth 1992;121:44–52.
60. Galkin O, Vekilov PG. Mechanisms of homogeneous nucleation of polymers of sickle cell anemia hemoglobin in deoxy state. J Mol Biol 2004;336:43–59. [PubMed: 14741202]
61. Borchers, H., editor. Springer; Berlin, Germany: 1955.
62. Chernov, AA.; Komatsu, H. Principles of crystal growth in protein crystallization. In: van der Eerden, JP.; Bruinsma, OSL., editors. Science and Technology of Crystal Growth. Kluwer Academic; Dordrecht, The Netherlands: 1995. p. 329-353.
63. Dunitz JD. The entropic cost of bound water in crystals and biomolecules. Science 1994;264:670. [PubMed: 17737951]
64. Eisenberg, D.; Crothers, D. Physical Chemistry with Applications to Life Sciences. The Benjamin/Cummins Publishing Company, Inc; Menlo Park, CA: 1979.
65. Choudhury N, Pettitt BM. On the mechanism of hydrophobic association of nanoscopic solutes. J Am Chem Soc 2005;127:3556–3567. [PubMed: 15755177]
66. Choudhury N, Pettitt BM. Dynamics of water trapped between hydrophobic solutes. J Phys Chem, B 2005;109:6422–6429. [PubMed: 16851715]
67. Lum K, Chandler D, Weeks JD. Hydrophobicity at small and large length scales. J Phys Chem, B 1999;103:4570–4577.
68. Vekilov PG, Kuznetsov YG, Chernov AA. Interstep interaction in solution growth; (101) ADP face. J Cryst Growth 1992;121:643–655.
69. Reviakine I, Georgiou DK, Vekilov PG. Capillarity effects on the crystallization kinetics: insulin. J Am Chem Soc 2003;125:11684–11693. [PubMed: 13129373]

70. Georgiou DK, Vekilov PG. A fast response mechanism for insulin storage in crystals may involve kink generation by association of 2D clusters. Proc Natl Acad Sci USA 2006;103:1681–1686. [PubMed: 16446456]

71. Bridges KR, Barabino GD, Brugnara C, Cho MR, Christoph GW, Dover G, et al. A multiparameter analysis of sickle erythrocytes in patients undergoing hydroxyurea therapy. Blood 1996;88:4701–4710. [PubMed: 8977264]

72. Platt OS, Orkin SH, Dover G, Beardsley GP, Miller B, Nathan DG. Hydroxyurea enhances fetal hemoglobin production in sickle cell anemia. J Clin Invest 1984;74:652–656. [PubMed: 6205021]

73. Brugnara C. Therapeutic strategies for prevention of sickle cell dehydration. Blood Cells Mol Diseases 2001;27:71–80.

74. Bolen DW. Protein stabilization by naturally occurring osmolytes. Methods Mol Biol 2001;168:17–36. [PubMed: 11357625]

75. Bennion BJ, Daggett V. The molecular basis for the chemical denaturation of proteins by urea. Proc Natl Acad Sci USA 2003;100:5142–5147. [PubMed: 12702764]

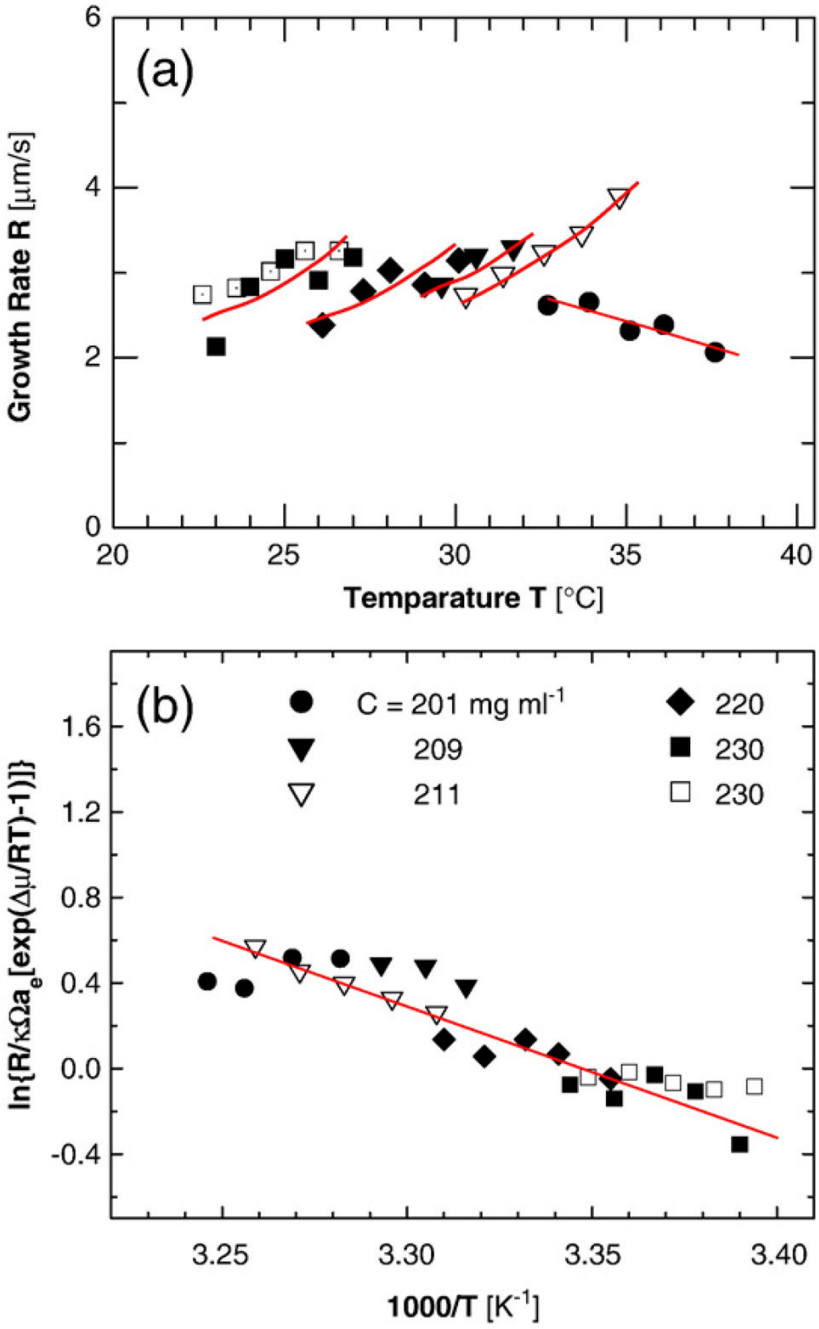

Fig. 1.

The kinetics of growth of the HbS fibers. (a) Growth rate *R* as a function of temperature at five HbS concentrations as indicated in (b), two independent data sets at C=230 mg ml^{-1} are shown (from Ref. 9). Lines for each HbS concentration are merely guides for the eyes. (b) Plot of data in (a) in Arrhenius coordinates, according to Eq. (5).

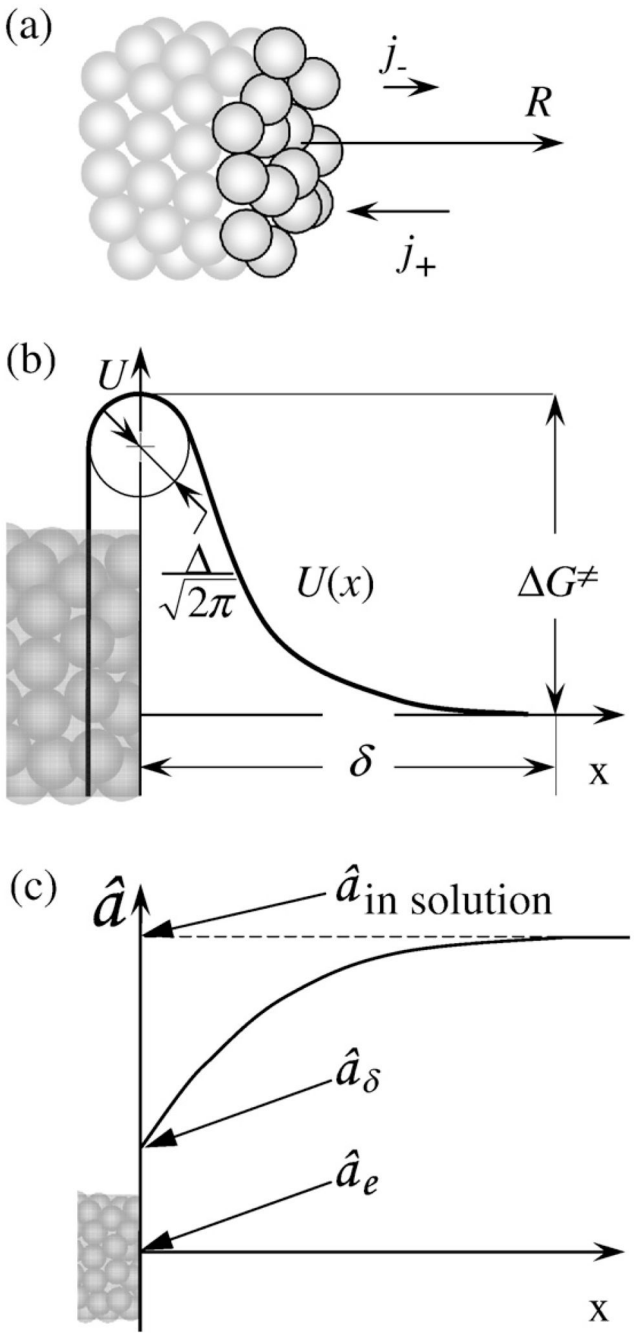

Fig. 2.

(a) Schematic representation of a growing fiber. HbS molecules at the growing edge are highlighted. (b) Schematic illustration of the free-energy relief $U(x)$ in front of the growing fiber; for the meaning of the symbols, see the text. Growth rate R, incoming flux j_+, and departing flux j_- of molecules in (a) and x-axis in (b) are directed along the fiber axis (c). Schematic representation of the distribution of HbS activity in front of a growing HbS polymer fiber. The x-scale in (c) is much coarser than that in (b).

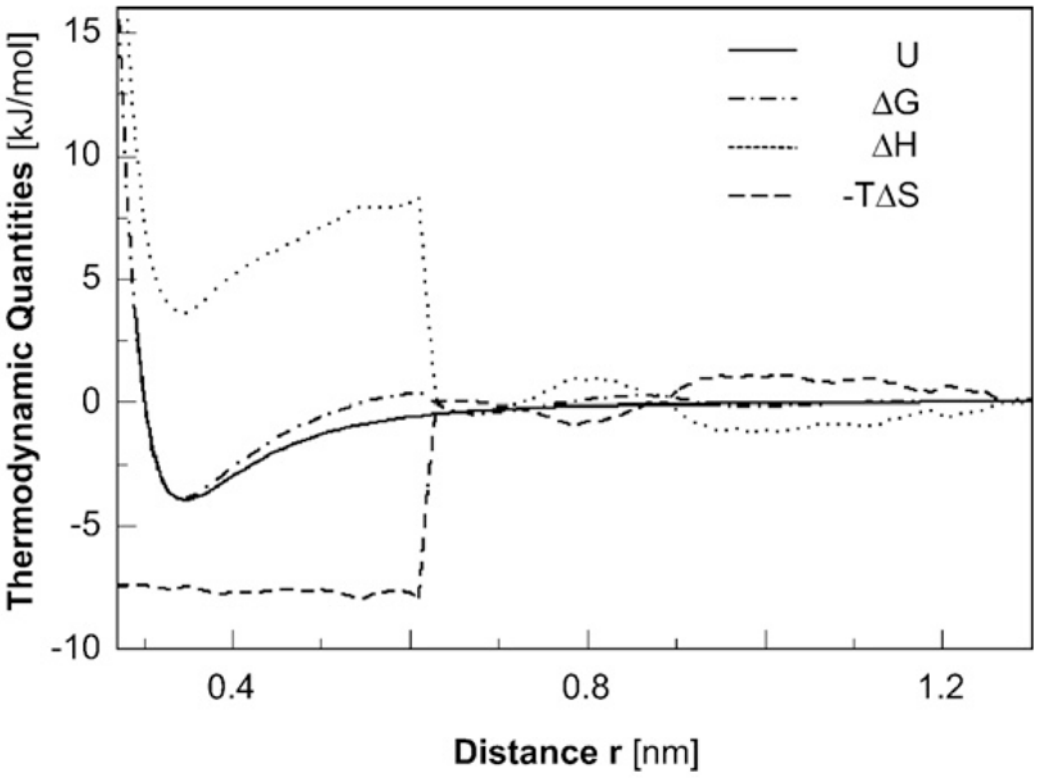

Fig. 3.

Interactions between idealized hydrophobic surfaces. Two graphene carbon surfaces of 60 atoms each are brought together in water via free-energy simulations.[55] Plotted as a function of the plate-to-plate separation r and normalized to represent the contribution per atom in the surfaces are the changes in energy U, the free energy ΔG, the enthalpy ΔH, and the entropic contribution $-T\Delta S$.